Ab initio molecular-dynamics study of structural, bonding, and dynamic properties of liquid B_2O_3 under pressure

Satoshi Ohmura and Fuyuki Shimojo
Department of Physics, Kumamoto University, Kumamoto 860-8555, Japan
(Received 17 October 2009; revised manuscript received 16 December 2009; published 19 January 2010)

The structural, bonding, and dynamic properties of liquid boron oxide, B_2O_3, under pressure are studied by *ab initio* molecular-dynamics simulations. To investigate the pressure dependence of the static structure, we obtain the structure factors, the pair distribution functions, and the distribution of the coordination numbers as a function of pressure. Planar BO_3 units are hardly deformed under pressures up to about 3 GPa, and the number of tetrahedral BO_4 units increases gradually under further compression. The bond-overlap populations and the Mulliken charges as well as the electronic density of states show that the covalent character is well preserved in the liquid state up to at least 200 GPa, although bond weakening occurs due to the increase in the coordination number. When the temperature is relatively low, the self-diffusion coefficients of boron and oxygen have a maximum at about 10 GPa because the concerted reactions, which enhance the atomic diffusion, occur more frequently with the increase in pressure below 10 GPa and are suppressed at higher pressures. The maximum behavior of the diffusivity becomes weaker with increasing temperature. A remarkable feature of the dynamic properties is that, under higher pressures over 20 GPa, the diffusivity of oxygen becomes much smaller than that of boron, regardless of temperature, while the former is slightly larger than the latter at lower pressures. Detailed discussions on the microscopic origin of this anomalous pressure dependence of the diffusivity are given.

DOI: 10.1103/PhysRevB.81.014208 PACS number(s): 61.20.Ja, 66.10.−x, 71.15.Pd

I. INTRODUCTION

Crystalline boron oxide (B_2O_3) in ambient conditions has a trigonal unit cell in which each boron atom is coordinated to three oxygen atoms with strong single bonds forming a triangular BO_3 unit, and each oxygen atom is twofold coordinated to boron atoms.[1,2] Under compression, a high-pressure phase appears at a pressure of about 6.5 GPa.[3,4] This structure has an orthorhombic unit cell which consists of interconnected BO_4 tetrahedral units with six- and eight-membered rings. Each boron atom bonds to four oxygen atoms to form a distorted tetrahedron with one short bond and three longer bonds. This reflects the fact that one third of the oxygen atoms are still twofold coordinated to boron atoms and the remaining have threefold coordination. In the vitreous state under pressures up to approximately 10 GPa, the coordination numbers are essentially unchanged while the planarity of the BO_3 units is lost with increasing pressure.[5] Fourfold-coordinated boron atoms appear at higher pressures and increase gradually with increasing pressure.[5,6]

It is well known that the transport properties of vitreous B_2O_3 (v-B_2O_3) are largely affected by the addition of alkali oxides.[7] Whereas the ionic conductivity of v-B_2O_3 without doped impurities is very small, it increases drastically with increasing the amount of alkali oxides added. Due to the presence of alkali elements as well as excess oxygen atoms, some of the covalent bonds between boron and oxygen atoms are broken. As a result, the network structure of v-B_2O_3, consisting of threefold-coordinated boron and twofold-coordinated oxygen atoms, is considerably modified by the doping.[8] It is, therefore, considered that these changes in the structural and bonding properties determine the transport properties of borate glasses and enhance the ionic conductivity. In this way, the atomic dynamics in B_2O_3 is directly influenced by the modification of the networks of B-O bonds. Since the local structure of v-B_2O_3 is modified by compression as described above, its dynamic properties are expected to change with pressure.

Although many studies on the properties of crystalline and vitreous B_2O_3 have been reported, there are few on liquid B_2O_3. It is known that the local coordination around each atom remains the same upon melting at atmospheric pressure,[9] i.e., boron atoms are predominantly threefold coordinated to oxygen atoms, and most of oxygen atoms bridge two adjacent boron atoms. However, the main difference of the liquid state from the crystalline and vitreous states comes from the fact that the covalent bonds must be rearranged with long-range atomic diffusion even without doped impurities. Recent first-principles investigation of the structural and bonding properties of liquid B_2O_3 (Ref. 10) has revealed that, under ambient conditions, a nonbridging oxygen double bonded to a twofold-coordinated boron is always involved with atomic diffusion accompanied by rearrangement of the covalent bonds to reduce the formation energy of the overcoordination defects.

Concerning the effects of pressure on the structure of the liquid state, the position of the first x-ray diffraction peak has been measured as a function of pressure up to about 5 GPa.[11] The transport properties of liquid B_2O_3 under pressure have been studied by quenching experiments[12] and computer simulations[13] with an empirical interatomic potential. The former has revealed that the viscosity of the undercooled melt decreases with increasing pressure up to 8 GPa. The latter has shown that the diffusivity of atoms is enhanced by pressure below 15 GPa, as in other covalent liquids, such as SiO_2 and GeO_2.[14,15] It is, however, unclear how the rearrangement process of the covalent bonds is affected by compression.

In this paper, we investigate the structural, electronic, and dynamic properties of liquid B_2O_3 under pressure by *ab initio* molecular-dynamics (MD) simulations with interatomic forces calculated quantum mechanically. So far, several first-principles studies for crystalline[16–19] and vitreous[5,20,21] B_2O_3 under ambient and high pressures have been reported. However, the liquid properties under pressure have not been investigated yet from first principles. The purposes of our study are (1) to clarify the pressure-induced structural change in liquid B_2O_3, (2) to elucidate the effects of pressure on the electronic properties, and (3) to discuss the mechanism of atomic diffusion accompanied by the B-O bond exchange under pressure. Although the major results for the dynamic properties have been reported earlier,[22] this paper provides a full description of the calculated results including the structural and electronic properties.

II. METHOD OF CALCULATION

In our MD simulations, a system of 120 (48B+72O) atoms in a cubic supercell was used under periodic boundary conditions. The equations of motion for atoms were solved via an explicit reversible integrator[23] with a time step of $\Delta t = 1.2$ fs. The atomic forces were obtained from the electronic states calculated by the projector-augmented-wave method[24,25] within the framework of density-functional theory. The generalized gradient approximation[26] was used for the exchange-correlation energy. The plane-wave cutoff energies are 30 and 200 Ry for the electronic pseudowave functions and the pseudocharge density, respectively. The energy functional was minimized using an iterative scheme.[27,28] Projector functions are generated for the $2s$ and $2p$ states of B and O. The Γ point was used for Brillouin-zone sampling.

As described in the previous paper,[10] we obtained a liquid state at density of 1.69 g/cm^3 and temperature of 2500 K. The density was determined from the extrapolation of the experimental data[29] obtained up to 1500 K. The temperature of 2500 K was chosen so as not only to be sufficiently high to maintain the liquid state even at the high pressures but also in order to observe enough number of atomic-diffusion events to analyze the diffusion mechanism in a statistically meaningful way within a limited amount of simulation time. Some simulations were performed at a higher temperature of 3500 K for the discussion of the temperature dependence. To determine the density of the liquid state under pressure, a constant-pressure MD simulation[30] was performed for 2.4 ps at each given pressure. Using the time-averaged density, the static and diffusion properties were investigated by MD simulations in the canonical ensemble.[31,32] The time-averaged pressure[33,34] was calculated at each density, and we obtained the density-pressure relation as shown in Fig. 1. The thermodynamic states investigated in this study cover a density range from 1.69 to 4.74 g/cm^3, and a pressure range from 1.4 to 198.8 GPa. The quantities of interest were obtained by averaging over 14.4–21.6 ps to achieve good statistics after the initial equilibration, which takes at least 2.4 ps.

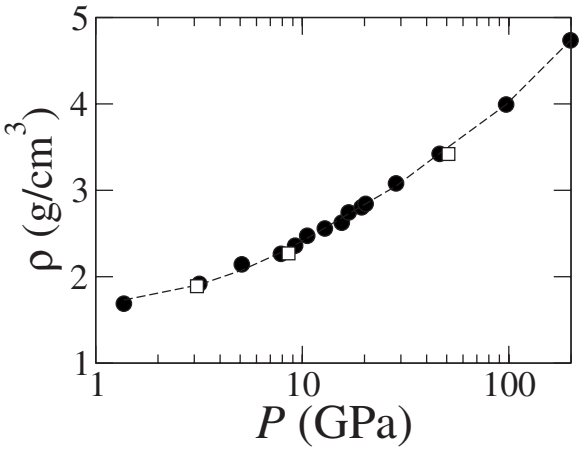

FIG. 1. Pressure dependence of the density of liquid B_2O_3 at 2500 K (solid circles) and 3500 K (open squares).

III. RESULTS AND DISCUSSION

A. Structure factor

Figure 2 shows the pressure dependence of the structure factors of liquid B_2O_3. The solid and dashed lines display the neutron and x-ray structure factors, $S_n(k)$ and $S_x(k)$, respectively. $S_n(k)$ is calculated from the partial structure factors

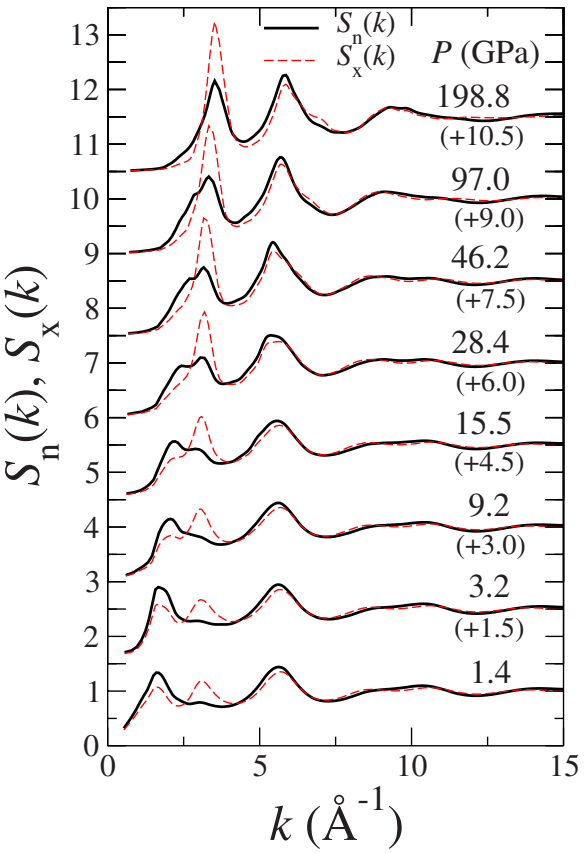

FIG. 2. (Color online) Pressure dependence of the total structure factors. The solid and dashed lines show the neutron and x-ray structure factors, $S_n(k)$ and $S_x(k)$, respectively. The curves are shifted vertically as indicated by the figures in parentheses.

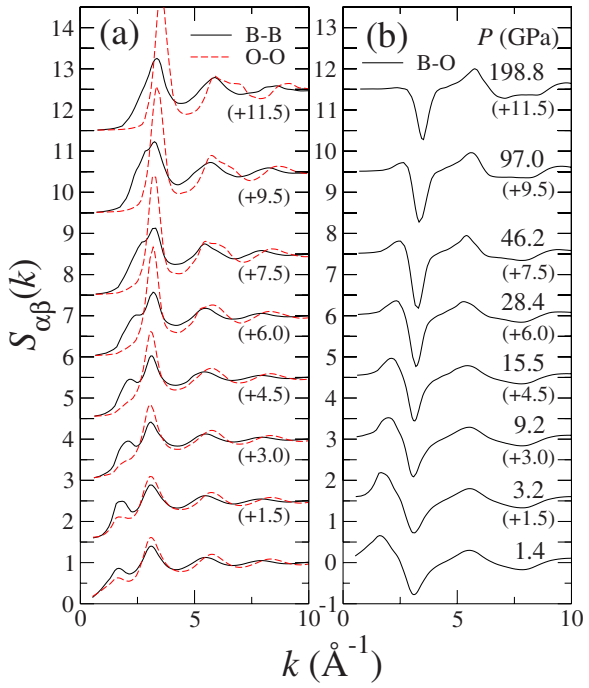

FIG. 3. (Color online) Pressure dependence of the partial structure factors $S_{\alpha\beta}(k)$. (a) The solid and dashed lines show $S_{\mathrm{BB}}(k)$ and $S_{\mathrm{OO}}(k)$, respectively. (b) The solid lines show $S_{\mathrm{BO}}(k)$. The curves are shifted vertically as indicated by the figures in parentheses.

$S_{\alpha\beta}(k)$, shown in Fig. 3, with the neutron-scattering lengths, and $S_{\mathrm{x}}(k)$ is obtained from $S_{\alpha\beta}(k)$ with the x-ray scattering factors. At pressures below 10 GPa, clear peaks exist at about $k=1.6$ and 6.0 Å^{-1} in the profiles of $S_{\mathrm{n}}(k)$ and $S_{\mathrm{x}}(k)$. Note that the overall profile of $S_{\mathrm{n}}(k)$ in this pressure range is consistent with the experimental $S_{\mathrm{n}}(k)$ of the vitreous state.[35] While only $S_{\mathrm{x}}(k)$ has another peak at about 3.2 Å^{-1} at lower pressures, the corresponding peak grows in $S_{\mathrm{n}}(k)$ at higher pressures. With increasing pressure, the peak at about $k=1.6$ Å^{-1} shifts to larger k, and merge into the peak at about $k=3.2$ Å^{-1} in both $S_{\mathrm{n}}(k)$ and $S_{\mathrm{x}}(k)$. This shift of the peak at about $k=1.6$ Å^{-1} in $S_{\mathrm{x}}(k)$ is in agreement with that observed by x-ray scattering experiments[11] up to 5 GPa. The peak at about $k=6.0$ Å^{-1} also becomes higher at higher pressures.

Figure 3 shows the Ashcroft-Langreth partial structure factors $S_{\alpha\beta}(k)$. The pressure dependence of the profiles of $S_{\mathrm{n}}(k)$ and $S_{\mathrm{x}}(k)$ is well understood from $S_{\alpha\beta}(k)$. At lower pressures, both $S_{\mathrm{BB}}(k)$ and $S_{\mathrm{OO}}(k)$ have the three peaks at about $k=1.6$, 3.2, and 6.0 Å^{-1}, which give the corresponding peaks in $S_{\mathrm{n}}(k)$ and $S_{\mathrm{x}}(k)$. Because of the cancellation due to the existence of a negative dip in $S_{\mathrm{BO}}(k)$, no clear peak appears in $S_{\mathrm{n}}(k)$ around $k=3.2$ Å^{-1}. With increasing pressure, the peak at about $k=1.6$ Å^{-1} shifts to larger k in $S_{\mathrm{BB}}(k)$ and $S_{\mathrm{BO}}(k)$ while it disappears around 10 GPa in $S_{\mathrm{OO}}(k)$. At the wave vector of about $k=3.2$ Å^{-1}, the peaks grow largely in $S_{\mathrm{BB}}(k)$ and $S_{\mathrm{OO}}(k)$ whereas the dip changes only a little in $S_{\mathrm{BO}}(k)$ with pressure. Therefore, the peaks of $S_{\mathrm{n}}(k)$ and $S_{\mathrm{x}}(k)$ grow at the corresponding k when the pressure increases. At higher pressures, the peak of $S_{\mathrm{OO}}(k)$ is much higher than that of $S_{\mathrm{BB}}(k)$.

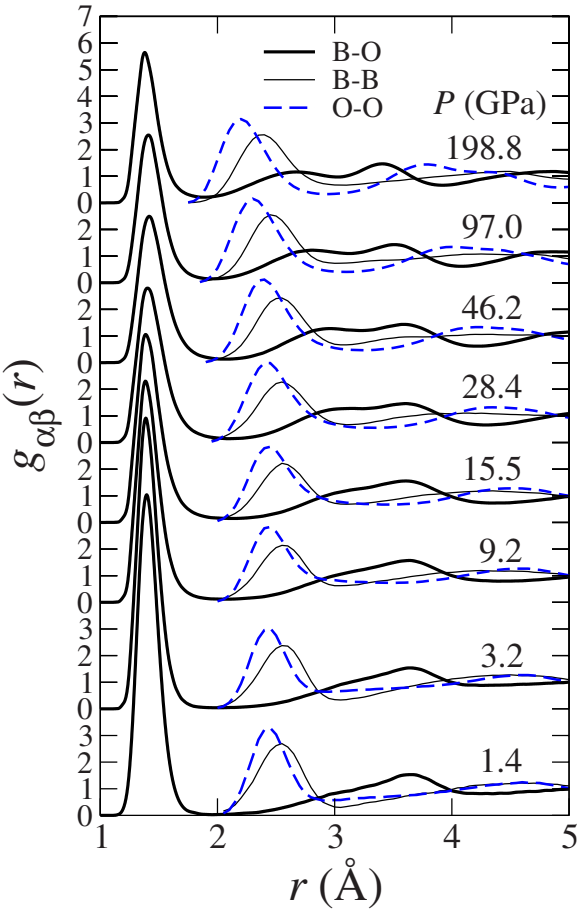

FIG. 4. (Color online) Pressure dependence of the partial pair distribution functions $g_{\alpha\beta}(r)$. The thick solid, thin solid, and thick dashed lines show $g_{\mathrm{BO}}(r)$, $g_{\mathrm{BB}}(r)$, and $g_{\mathrm{OO}}(r)$, respectively.

B. Pair distribution function

The pressure dependence of the partial pair distribution functions $g_{\alpha\beta}(r)$ is displayed in Fig. 4. In $g_{\mathrm{BO}}(r)$, a sharp first peak exists at about 1.4 Å over all pressures, and becomes more asymmetric with increasing pressure. There are no homopolar bonds in liquid B_2O_3 under pressure, as $g_{\mathrm{BB}}(r)$ and $g_{\mathrm{OO}}(r)$ are zero over the r range of the first peak of $g_{\mathrm{BO}}(r)$ even at higher pressures. Note that a very broad peak appears around 3 Å in the profile of $g_{\mathrm{BO}}(r)$ when the pressure approaches about 30 GPa. This peak is related to the appearance of ring structures at higher pressures.

Figures 5(a)–5(c) show the pressure dependence of the nearest-neighbor distances $r_{\alpha\beta}$ between α-and β-type atoms, which were obtained from the first-peak positions of $g_{\alpha\beta}(r)$. The pressure dependence of the average oxygen coordination number N_{BO} around B atoms is shown in Fig. 5(d). We calculated N_{BO} by the integration of $4\pi r^2 n_{\mathrm{O}} g_{\mathrm{BO}}(r)$ from $r=0$ to 1.9 Å, which was determined with reference to the first-minimum position at the lowest pressure,[36] where n_{O} is the number density of O atoms. The local bonding nature remains almost unchanged up to about 3 GPa because all three $r_{\alpha\beta}$ and N_{BO} have nearly no pressure dependence. This means that the system is compressed by decreasing the empty space. For $P>3$ GPa, N_{BO} increases gradually with

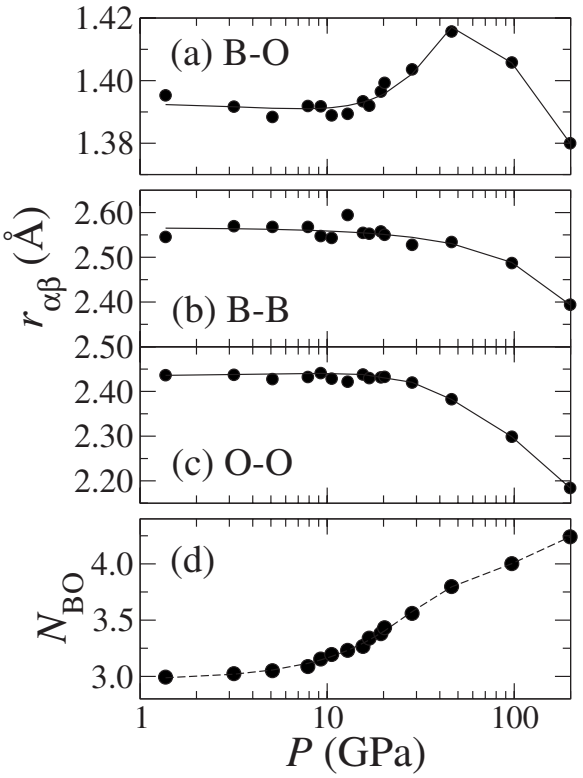

FIG. 5. Pressure dependence of the nearest-neighbor distances $r_{\alpha\beta}$ for α-β=(a) B-O, (b) B-B, and (c) O-O. (d) Pressure dependence of the oxygen coordination number N_{BO} around boron atoms.

increasing pressure while r_{BO} still keeps its value constant up to about 10 GPa, which is consistent with the fact that the asymmetry of the first peak of $g_{BO}(r)$ becomes larger. With further compression for $P>10$ GPa, r_{BO} increases with pressure and has a maximum at about 50 GPa while r_{BB} and r_{OO} decrease monotonically. Accompanying these changes, N_{BO} increases and approaches four at about 100 GPa, indicating that the local structure changes largely with pressure. Note that the difference between r_{BB} and r_{OO} becomes larger with increasing pressure. This implies that the average B-O-B and O-B-O angles change differently under compression because r_{BB} and r_{OO} reflect these angles.

C. Coordination-number distribution

Figure 6 shows the pressure dependence of the coordination-number distribution $f^{(n)}_{\alpha\beta}$, which is the ratio of $N^{(n)}_{\alpha\beta}/N_\alpha$, where $N^{(n)}_{\alpha\beta}$ is the number of α-type atoms coordinated to n β-type atoms and N_α is the total number of α-type atoms. To obtain $N^{(n)}_{\alpha\beta}$, the same cutoff distance $R=1.9$ Å was used as in the calculation of N_{BO}. From Fig. 6, we see that liquid B_2O_3 consists mainly of BO_3 units connected by bridging O atoms under pressures up to about 3 GPa, and the BO_4 units increase gradually with increasing pressure for $P>3$ GPa. $f^{(3)}_{BO}$ and $f^{(4)}_{BO}$ are exchanged for each other at about 25 GPa while $f^{(2)}_{OB}$ and $f^{(3)}_{OB}$ are interchanged at a higher pressure of about 50 GPa. At about 100 GPa, the number of fourfold-coordinated B atoms approaches about 90% and about 5% of B atoms have fivefold coordination. Under further compression up to about 200 GPa, one fourth of the B atoms have fivefold coordination, and instead fourfold-coordinated B atoms decrease. Also, fourfold-coordinated O atoms appear under such high pressures whereas twofold-coordinated O atoms still exist.

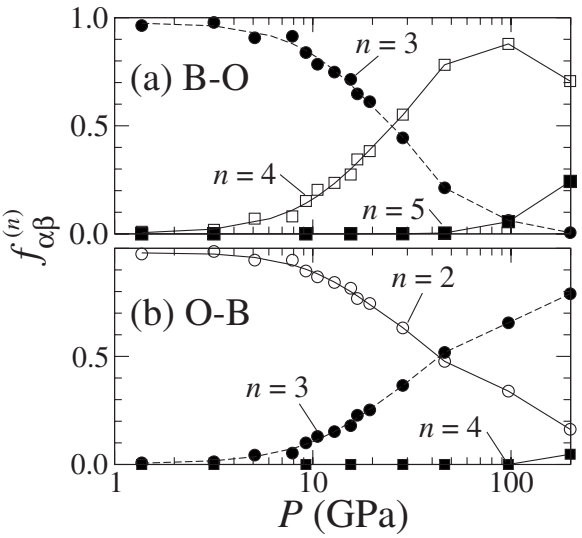

FIG. 6. Pressure dependence of the coordination-number distribution $f^{(n)}_{\alpha\beta}$ for α-β=(a) B-O and (b) O-B.

D. Electronic density of states

Figures 7 and 8 show the pressure dependence of the total electronic density of states (DOS), $D(E)$, and the angular momentum l-dependent partial DOS, $D^l_\alpha(E)$, for α-type atoms, respectively. $D(E)$ is related to $D^l_\alpha(E)$ as $D(E)=\Sigma_\alpha c_\alpha \Sigma_l D^l_\alpha(E)$, where c_α is the number concentration of α-type atoms. In $D(E)$, there are two segments below the Fermi level ($E=0$) over all pressures. The peak at around $E=-22$ eV shifts to lower energies and its energy range spreads with compression. Another segment consists of a large peak at about $E=-4$ eV and a shoulder around $E=-9$ eV at lower pressures. Note that the peak at about $E=-4$ eV originates from the lone-pair (LP) nonbonding p states around O atoms [see Fig. 8(b)]. This peak becomes lower with increasing pressure and its height are comparable to the shoulder at higher pressures, which means that some of the LP states are lost around O atoms. As was seen in Fig. 6, fourfold-coordinated B and threefold-coordinated O atoms increase with increasing pressure, and it is, therefore, obvious that the electrons in the LP states are used to form new bonds between B and O atoms. The $2s$ and $2p$ orbitals are hybridized around B atoms at all pressures as shown in Fig. 8(a).

E. Bond-overlap population

We used population analysis[37,38] to clarify the change in the bonding properties due to compression. By expanding the electronic wave functions in an atomic-orbital basis set, we obtained the overlap population O_{ij} between the ith and jth atoms and the gross charge Q_i for the ith atom. O_{ij} gives a

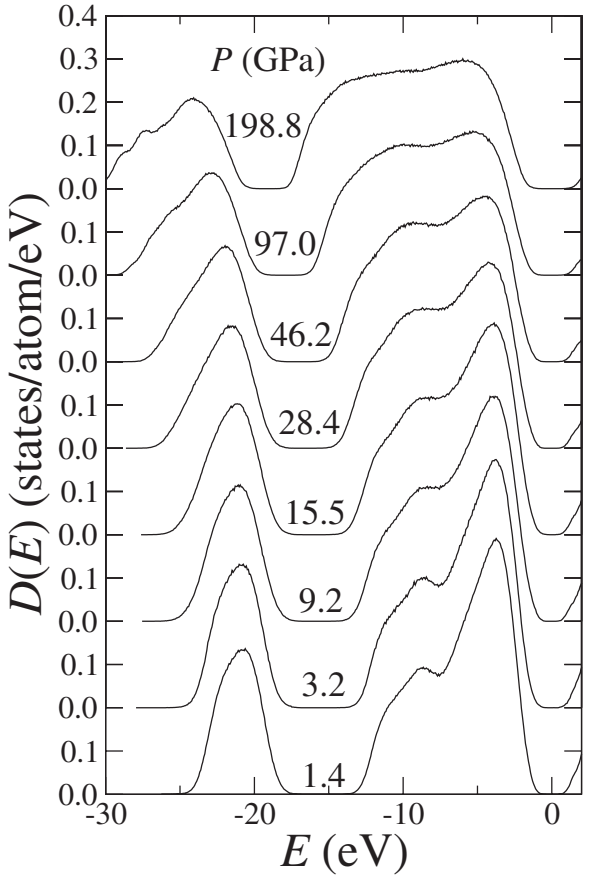

FIG. 7. Pressure dependence of the electronic density of states $D(E)$.

semiquantitative estimate of the strength of the covalentlike bonding between atoms, and Q_i is a quantity that measures the ionicity of each atom. Figure 9 shows the time-averaged distribution $p_{\alpha\beta}(\bar{O})$ of the overlap populations $O_{i\in\alpha,j\in\beta}$. At all pressures, there is a clear peak at positive $\bar{O}$. This indicates that the covalent bond between B and O atoms is retained up to at least 200 GPa. The position of this peak is about $\bar{O}=0.75$ up to 15.5 GPa, which reflects the σ-type covalent B-O bonds in the BO_3 units. It shifts to lower $\bar{O}=0.6$ between 15.5 and 46.2 GPa, and is unchanged at pressures over 46.2 GPa. This pressure dependence of $p_{\alpha\beta}(\bar{O})$ reveals that the covalent B-O bonds become weak accompanying the increase in the BO_4 units. A clear peak also exists at negative $\bar{O}$, which comes from the interaction between the LP states around O atoms and the bonding states around B atoms. This peak grows with increasing pressure, reflecting the increase in interactions between O and B atoms.

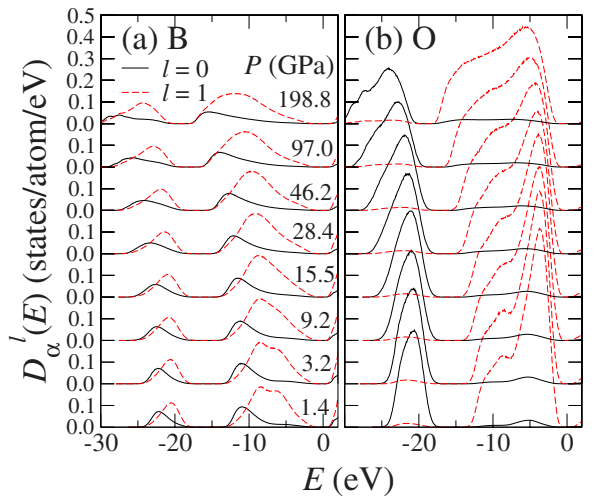

FIG. 8. (Color online) Pressure dependence of the angular momentum l-dependent partial electronic density of states $D_\alpha^l(E)$ for α=(a) B and (b) O atoms. The solid and dashed lines show $D_\alpha^l(E)$ for l=0 and 1, respectively.

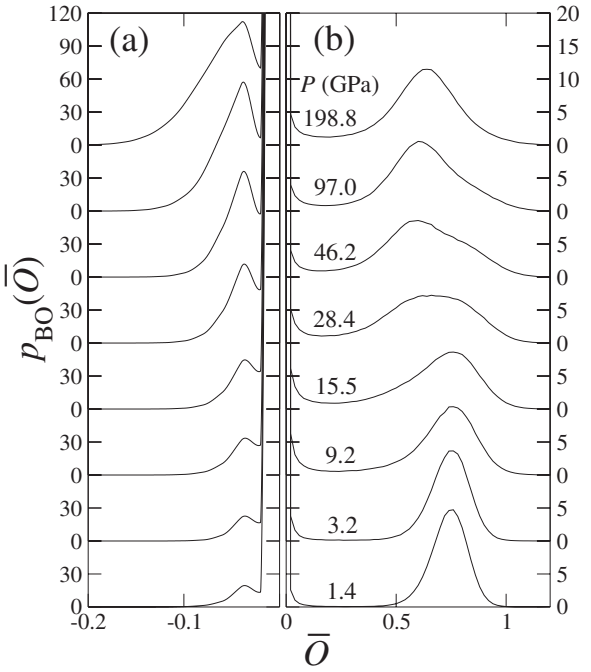

FIG. 9. Pressure dependence of the distribution of the bond-overlap populations $p_{\mathrm{BO}}(\bar{O})$ for (a) $\bar{O}<0$ and (b) $\bar{O}>0$

F. Mulliken charge

Figure 10 shows the time-averaged distributions $q_\alpha(Q)$ of the gross charges $Q_{i\in\alpha}$ for α-type atoms. The peak positions of $q_{\mathrm{B}}(Q)$ and $q_{\mathrm{O}}(Q)$ shift to smaller and larger Q, respectively, with increasing pressure, i.e., the electrons around O atoms are transferred toward B atoms. This is consistent with the fact that the spatial distribution of the electrons that form the LP states around O atoms at lower pressures spreads to form new B-O bonds with increasing pressure. We can see that $q_{\mathrm{O}}(Q)$ has a shoulder besides the peak at higher pressures over 46.2 GPa; the shoulder originates from twofold-coordinated O atoms while the peak comes from threefold-coordinated O atoms. On the other hand, $q_{\mathrm{B}}(Q)$ consists of only one peak for this pressure range because almost all B atoms have fourfold coordination.

G. Diffusivity

The pressure dependence of the mean-square displacements $d_\alpha(t)$ is shown in Fig. 11, where the solid and open

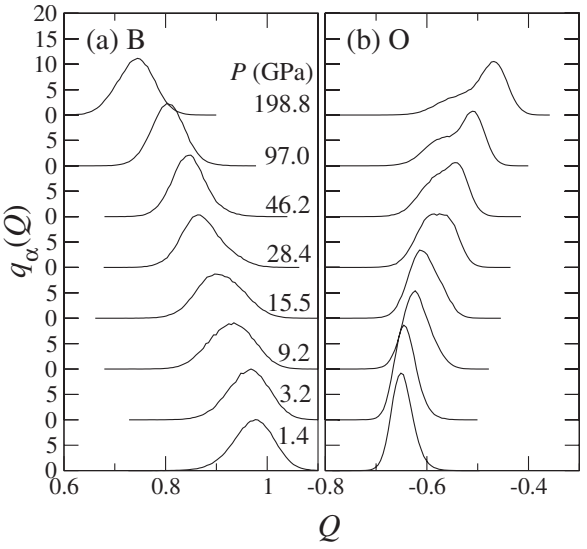

FIG. 10. Pressure dependence of the distribution of the gross charges $q_\alpha(Q)$ for α=(a) B and (b) O.

symbols show $d_B(t)$ and $d_O(t)$, respectively. $d_\alpha(t)$ is defined as $d_\alpha(t)=\Sigma_{i\in\alpha}\langle[r_i(t)-r_i(0)]^2\rangle/N_\alpha$, where $r_i(t)$ is the position of the ith atom at time t and the brackets $\langle\cdots\rangle$ mean average with respect to the time origin t=0. Both $d_B(t)$ and $d_O(t)$ have finite slopes, i.e., liquid states are reproduced by our simulations. Since the slopes of $d_B(t)$ and $d_O(t)$ increase when the pressure is increased from 1.4 to 9.2 GPa, we see that the atomic diffusion is enhanced by compression. Under further compression to 28.4 GPa, the slopes of $d_B(t)$ and $d_O(t)$ decrease. Note that the slope of $d_B(t)$ is larger than that of $d_O(t)$ at 28.4 GPa while $d_O(t)$ has a slightly larger slope at 1.4 and 9.2 GPa.

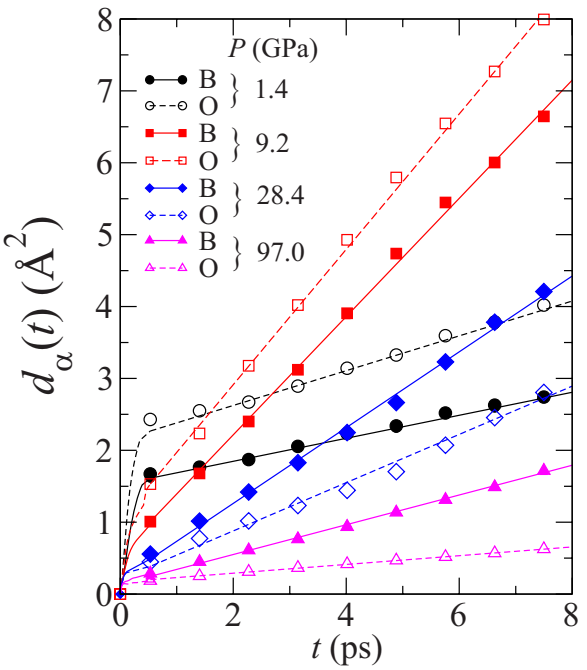

FIG. 11. (Color online) Pressure dependence of the mean-square displacements $d_\alpha(t)$. The solid and open symbols show $d_B(t)$ and $d_O(t)$, respectively.

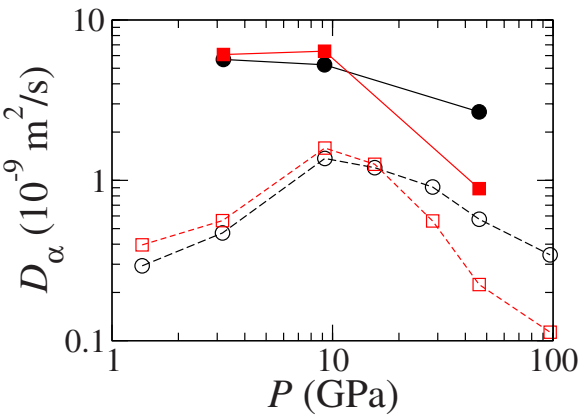

FIG. 12. (Color online) Pressure dependence of the diffusion coefficients D_α for α=B (circles) and O (squares) atoms. The open and solid symbols indicate D_α at temperatures of 2500 and 3500 K, respectively.

Figure 12 shows the diffusion coefficients D_α for α=B and O atoms as a function of pressure. They were estimated from the slopes of $d_\alpha(t)$. Clearly, liquid B_2O_3 has a diffusion maximum around 10 GPa at the temperature of 2500 K. (See the open symbols. The temperature dependence will be discussed later.) In the pressure range of $P<10$ GPa, both D_B and D_O increase with increasing pressure similarly to each other, which is consistent with the observed pressure dependence of the viscosity of the undercooled liquid.[12] While D_O has 10–20 % larger values than D_B under pressures up to about 10 GPa, D_B becomes more than two times larger than D_O when the pressure exceeds 20 GPa. At about 200 GPa, only a few oxygen-diffusion events were observed within the simulated time of about 17 ps, and it is hard to estimate D_O from $d_O(t)$ while $d_B(t)$ has a finite slope ($D_B\sim10^{-10}$ m^2/s).

H. Mechanism of atomic diffusion

The diffusion enhancement must be related to the weakening of the covalentlike interaction between atoms accompanying the increase in the coordination number, as in other covalent liquids.[14,15] In fact, we found that, in liquid B_2O_3 under pressures over 3 GPa, long-range atomic diffusion occurs by the usual concerted reactions as shown in Fig. 13 while the nonbridging O atoms are always involved in diffusion processes at lower pressures.[10] In Fig. 13, the time evolution of the bond-overlap populations $O_{ij}(t)$ associated with the B and O atoms of interest is displayed with snapshots of atomic configurations. As displayed in the snapshot at 0.09 ps, two BO_4 groups are generated as an intermediate by forming two new B-O bonds between adjoining BO_3 units, in contrast to the fact that only one BO_4 group is required to produce the nonbridging O atoms. The concerted reactions occur more frequently under higher pressures, which will result from the covalent-bond weakening due to the compression, and will enhance the atomic diffusion. We also observed that the reactions with the nonbridging O atoms decrease with increasing pressure and almost disappear for $P>10$ GPa.

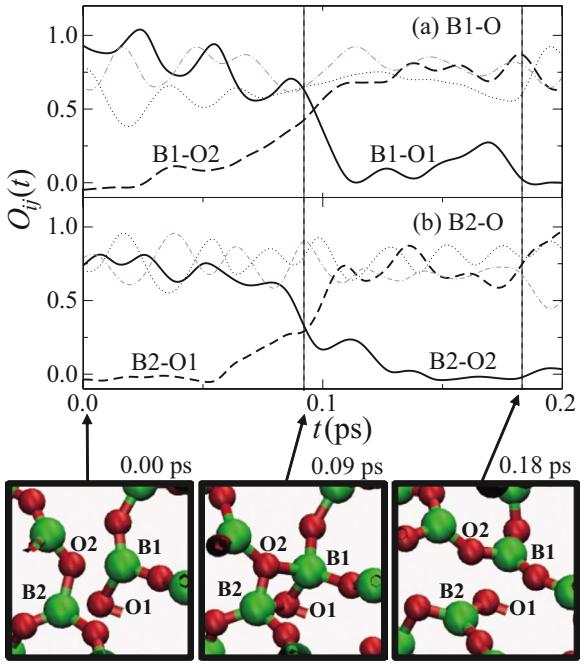

FIG. 13. (Color online) (Top panel) Time evolution of the bond-overlap populations $O_{ij}(t)$ for (a) i=B1, $j \in$ O and (b) i=B2, $j \in$ O in the process of bond switching with two BO_3 groups observed at 9.2 GPa. The thick solid and thick dashed lines show $O_{ij}(t)$ associated with the B (labeled as "B1" and "B2") and O (labeled as "O1" and "O2") atoms of interest. The thin lines show $O_{ij}(t)$ between the B1 or B2 atoms and their neighboring O atoms except O1 and O2. (Bottom panel) Atomic configurations at t =0.00, 0.09, and 0.18 ps. The large and small spheres show B and O atoms, respectively.

The concerted reactions as well as the reactions with the nonbridging O atoms involve equal numbers of B and O atoms, and therefore D_B and D_O would depend similarly to each other on pressure up to about 10 GPa as seen in Fig. 12. D_O has 10–20 % larger values than D_B, which may be due to the lower coordination number of O atoms.[22] The appearance of diffusion maximum is not surprising but quite natural in the covalent liquids. It is, however, unusual that the diffusivity of O atoms is reduced more quickly than that of B atoms with compression above 10 GPa. The important point is that, under pressures over 20 GPa, the number of fourfold-coordinated B atoms is much larger than that of threefold-coordinated B atoms, and, on the other hand, both twofold- and threefold-coordinated O atoms exist. As we have shown in the previous paper,[22] fourfold-coordinated B atoms can move toward neighboring twofold-coordinated O atoms through the threefold coordination with planar arrangement. In this diffusion process, only B atom diffuses between O atoms. Since several twofold-coordinated O atoms exist around each B atom even at high pressures over 20 GPa,[22] this type of diffusion process occurs rather frequently. On the other hand, the usual concerted reaction is suppressed at higher pressures because the number of threefold-coordinated B atoms decreases rapidly with increasing pressure for $P > 20$ GPa, which causes the quick decrease in D_O.

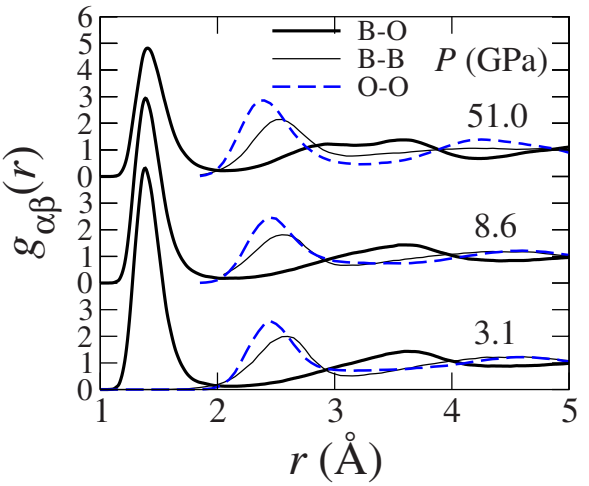

FIG. 14. (Color online) Pressure dependence of the partial pair distribution functions $g_{\alpha\beta}(r)$ at a high temperature of 3500 K. The thick solid, thin solid, and thick dashed lines show $g_{BO}(r)$, $g_{BB}(r)$, and $g_{OO}(r)$, respectively.

I. Temperature dependence

In order to investigate the effects of temperature on the properties of liquid B_2O_3 under pressure, some MD simulations were carried out at a higher temperature of 3500 K. Figure 14 shows the pressure dependence of $g_{\alpha\beta}(r)$ at 3500 K. From the comparison of each profile with the corresponding $g_{\alpha\beta}(r)$ at 2500 K (Fig. 4), we see that the first peaks of all $g_{\alpha\beta}(r)$ become broader because of the larger thermal motion of atoms. However, the peak positions and the average coordination numbers are almost unchanged. In this sense, the effects of the increase in pressure to ~50 GPa on the static structure would be more important than those of the increase in temperature from 2500 to 3500 K.

The pressure dependence of the diffusion coefficients D_α at 3500 K is shown in Fig. 12 together with that at 2500 K. The maximum behavior of the diffusivity becomes weaker or disappears when the temperature is higher. A similar temperature dependence has been seen in liquid SiO_2.[14] Note that the diffusivity of O atoms becomes much lower than that of B atoms with increasing pressure even at 3500 K. This is because B atoms will eventually have fourfold coordination with compression, regardless of temperature.

IV. SUMMARY

We have investigated the structural, bonding, and dynamic properties of liquid B_2O_3 under pressures up to about 200 GPa by *ab initio* molecular-dynamics simulations. The effects of compression on the static structure have been discussed based on the pressure dependence of the structure factors, the pair distribution functions, the nearest-neighbor distances, and the coordination-number distribution. The structure consists mainly of planar BO_3 units up to about 3 GPa, and the number of tetrahedral BO_4 units increases gradually under further compression. The number of fourfold-coordinated B atoms reaches a maximum of about 90% at about 100 GPa. Threefold-coordinated B atoms al-

most disappear at pressures over 50 GPa whereas twofold-coordinated O atoms still exist even under such high pressures. The bonding properties at each pressure have been examined by population analysis. It has been seen from the distribution of the bond-overlap populations that the covalent bonds weaken due to the structural change from BO_3 to BO_4 units. The pressure dependence of the mean-square displacements has shown that the diffusion maximum occurs at about 10 GPa when the temperature is relatively low. Regardless of temperature, the diffusivity of O atoms will eventually becomes much smaller than that of B atoms under higher pressures while the former is slightly larger than the latter at lower pressures. This is because the number of threefold-coordinated B atoms decreases rapidly with pressure and the concerted reaction is suppressed.

ACKNOWLEDGMENTS

The authors acknowledge useful discussions with Masaru Aniya. The present work was supported in part by a Grant-in-Aid for Scientific Research on Priority Area, "Nanoionics (439)" from the MEXT, Japan. The computation was carried out using the computer facilities at Research Institute for Information Technology, Kyushu University.

[1] G. E. Gurr, P. W. Montgomery, C. D. Knutson, and B. T. Gorres, Acta Crystallogr., Sect. B: Struct. Crystallogr. Cryst. Chem. **26**, 906 (1970).
[2] P. A. V. Johnson, A. C. Wright, and R. N. Sinclair, J. Non-Cryst. Solids **50**, 281 (1982).
[3] C. T. Prewitt and R. D. Shannon, Acta Crystallogr., Sect. B: Struct. Crystallogr. Cryst. Chem. **24**, 869 (1968).
[4] D. Nieto-Sanz, P. Loubeyre, W. Crichton, and M. Mezouar, Phys. Rev. B **70**, 214108 (2004).
[5] V. V. Brazhkin, Y. Katayama, K. Trachenko, O. B. Tsiok, A. G. Lyapin, E. Artacho, M. Dove, G. Ferlat, Y. Inamura, and H. Saitoh, Phys. Rev. Lett. **101**, 035702 (2008).
[6] S. K. Lee, P. J. Eng, H. K. Mao, Y. Meng, M. Newville, M. Y. Hu, and J. F. Shu, Nature Mater. **4**, 851 (2005).
[7] M. Massot and M. Balkanski, *Disorder in Condensed Matter Physics*, edited by J. A. Blackman and J. Taguena, (Oxford, New York, 1991), p. 74.
[8] *Optical Constants of Inorganic Glasses*, edited by A. M. Efimov (CRC, New York, 1995), p. 88.
[9] J. Sakowski and G. Herms, J. Non-Cryst. Solids **293-295**, 304 (2001).
[10] S. Ohmura and F. Shimojo, Phys. Rev. B **78**, 224206 (2008).
[11] V. V. Brazhkin, Y. Katayama, Y. Inamura, M. V. Kondrin, A. G. Lyapin, S. V. Popova, and R. N. Voloshin, JETP Lett. **78**, 393 (2003).
[12] V. V. Brazhkin and A. G. Lyapin, J. Phys.: Condens. Matter **15**, 6059 (2003).
[13] J. Diefenbacher and P. F. McMillan, J. Phys. Chem. A **105**, 7973 (2001).
[14] B. B. Karki, D. Bhattarai, and L. Stixrude, Phys. Rev. B **76**, 104205 (2007).
[15] V. Van Hoang, H. Zung, and N. T. Hai, J. Phys.: Condens. Matter **19**, 116104 (2007).
[16] A. Takada, C. R. A. Catlow, J. S. Lin, G. D. Price, M. H. Lee, V. Milman, and M. C. Payne, Phys. Rev. B **51**, 1447 (1995).
[17] D. Li and W. Y. Ching, Phys. Rev. B **54**, 13616 (1996).
[18] U. Engberg, Phys. Rev. B **55**, 2824 (1997).
[19] M. M. Islam, T. Bredow, and C. Minot, Chem. Phys. Lett. **418**, 565 (2006).
[20] T. Uchino and T. Yoko, J. Chem. Phys. **105**, 4140 (1996).
[21] P. Umari and A. Pasquarello, Phys. Rev. Lett. **95**, 137401 (2005).
[22] S. Ohmura and F. Shimojo, Phys. Rev. B **80**, 020202(R) (2009).
[23] M. Tuckerman, B. J. Berne, and G. J. Martyna, J. Chem. Phys. **97**, 1990 (1992).
[24] P. E. Blöchl, Phys. Rev. B **50**, 17953 (1994).
[25] G. Kresse and D. Joubert, Phys. Rev. B **59**, 1758 (1999).
[26] J. P. Perdew, K. Burke, and M. Ernzerhof, Phys. Rev. Lett. **77**, 3865 (1996).
[27] G. Kresse and J. Hafner, Phys. Rev. B **49**, 14251 (1994).
[28] F. Shimojo, R. K. Kalia, A. Nakano, and P. Vashishta, Comput. Phys. Commun. **140**, 303 (2001).
[29] P. B. Macedo, W. Capps, and T. A. Litovitz, J. Chem. Phys. **44**, 3357 (1966).
[30] G. J. Martyna, D. J. Tobias, and M. L. Klein, J. Chem. Phys. **101**, 4177 (1994).
[31] S. Nosé, Mol. Phys. **52**, 255 (1984).
[32] W. G. Hoover, Phys. Rev. A **31**, 1695 (1985).
[33] O. H. Nielsen and R. M. Martin, Phys. Rev. B **32**, 3780 (1985).
[34] A. Dal Corso and R. Resta, Phys. Rev. B **50**, 4327 (1994).
[35] A. C. Hannon, D. I. Grimley, R. A. Hulme, A. C. Wright, and R. N. Sinclair, J. Non-Cryst. Solids **177**, 299 (1994).
[36] Since the first peak of $g_{BO}(r)$ is rather asymmetric, we do not calculate N_{BO} as the integration up to r_{BO} (times two).
[37] F. Shimojo, A. Nakano, R. K. Kalia, and P. Vashishta, Phys. Rev. E **77**, 066103 (2008).
[38] R. S. Mulliken, J. Chem. Phys. **23**, 1841 (1955).